A new hard x-ray spectrometer for runaway electron measurements in tokamaks

OPEN ACCESS
IOP Publishing
Measurement Science and Technology
Meas. Sci. Technol. **34** (2023) 085501 (10pp)
https://doi.org/10.1088/1361-6501/acd46c

A new hard x-ray spectrometer for runaway electron measurements in tokamaks

A Dal Molin[1,*], M Nocente[2], M Dalla Rosa[2], E Panontin[2], D Rigamonti[1], M Tardocchi[1], A Shevelev[3], E Khilkevitch[3], M Iliasova[3], L Giacomelli[1], G Gorini[2], E Perelli Cippo[1], F D'Isa[4], G Pautasso[4], G Papp[4], G Tardini[4], E Macusova[5], J Cerovsky[5,6], O Ficker[5,6], M Salewski[7], V Kiptily[8], the EUROfusion MST1 Team[9], the COMPASS Team[5] and the ASDEX Upgrade Team[10]

[1] Istitute for Plasma Science and Technology ISTP, CNR, Milan, Italy
[2] University of Milano-Bicocca, Milan, Italy
[3] IOFFE Physical Technical Institute, Saint Petersburg, Russia
[4] Max-Planck-Intitut für Plasmaphysik, Garching bei München, Germany
[5] Institute of Plasma Physics of the CAS, Prague, Czech Republic
[6] FNSPE, Czech Technical University, Prague, Czech Republic
[7] Department of Physics, Technical University of Denmark, Lyngby, Denmark
[8] Culham Centre for Fusion Energy of UKAEA, Culham Science Centre, Abingdon, United Kingdom

E-mail: andrea.dalmolin@istp.cnr.it

Received 4 April 2023, revised 5 May 2023
Accepted for publication 11 May 2023
Published 23 May 2023

Abstract

Runaway electron gamma-ray detection system, a novel hard x-ray (HXR) spectrometer optimized for bremsstrahlung radiation measurement from runaway electrons in fusion plasmas, has been developed. The detector is based on a 1'×1' $LaBr_3$:Ce scintillator crystal coupled with a photomultiplier tube. The system has an energy dynamic range exceeding 20 MeV with an energy resolution of 3% at 661.7 keV. The detector gain is stable even under severe loads, with a gain shift that stays below 3% at HXR counting rates in excess of 1 MCps. The performance of the system enables unprecedented studies of the time-dependent runaway electron energy distribution function, as shown in recent runaway electron physics experiments at the ASDEX Upgrade and COMPASS tokamaks.

Keywords: nuclear instruments and methods for hot plasma diagnostics, x-ray detectors, runaway electrons

(Some figures may appear in colour only in the online journal)

[9] See the author list of B. Labit *et al* 2019 *Nucl. Fusion* **59** 086020.
[10] See the author list of H. Meyer *et al* 2019 *Nucl. Fusion* **59** 112014.
[*] Author to whom any correspondence should be addressed.

1. Introduction

Undesired runaway electron (RE) generation remains one of the major challenges to the success of net fusion energy tokamak operation [1–3]. During a disruption, a significantly large portion of the energy stored in the internal magnetic field can be efficiently transferred to the runaway electron beam via the generation of large toroidal electric fields. Once confinement is lost, these highly energetic particles can impact and damage plasma-facing components, hindering operation. In the worst case scenario, the damage to the machine vessel may be significant enough to cause a long shutdown period to enable repairs that may last several months [4].

To avoid these extreme scenarios, extensive research is currently being carried out by the tokamak community [5]. A large fraction of this work is carried out on the tokamaks ASDEX Upgrade (AUG) and COMPASS where runaway electron beams are purposely generated to study the phenomenon [6–8].

During the generation process, runaway electrons can be accelerated to energies of the order of several MeV. These relativistic particles interact with the post-disruption plasma and emit hard x-rays (HXR) from bremsstrahlung radiation up to several MeVs. Information on the runaway electron energy distribution function can be extracted measuring this hard x-ray emission [9]. In particular, the study of the RE energy distribution is crucial to understand runaway electron formation, to validate first-principle models and to evaluate the effectiveness of different runaway electron mitigation techniques such as massive gas injection (MGI) [6, 10], shattered pellet injection [5] and magnetic resonant perturbation [11, 12].

The measurement of the runaway bremsstrahlung radiation is challenging. When runaway electrons are generated in a medium-size or a large-size tokamak, the resulting bremsstrahlung radiation usually covers a large range of energies from a few keV up to a few tens of MeV. Moreover, radiation fluxes up to several million photons per square centimetre per second can reach the detector even when it is placed at several meters from the centre of the plasma cross section. Finally, the runaway electron distribution function can rapidly change over time scales of a few milliseconds. The challenging nature of runaway electron bremsstrahlung measurement requires the development of fast diagnostics specifically designed for this task [13–15].

In this work, we present a new hard x-ray spectrometer optimized for runaway electron bremsstrahlung measurements: the Runaway Electron GAmma-Ray Detection System (REGARDS).

2. The runaway electron gamma-ray detection system

The REGARDS is a portable hard x-ray spectrometer specifically designed to measure the bremsstrahlung radiation emitted by the interaction of the runaway electron beam with the post-disruption plasma. It is based on the design of a former detector used for exploratory measurements at the AUG tokamak [16], but with significant improvements mostly concerning its data acquisition and gain control systems, as well as shielding from background radiation, thus enabling measurements of the RE energies with a higher degree of fidelity at the 10^6 counts per second (MCps) counting rates often observed during experiments.

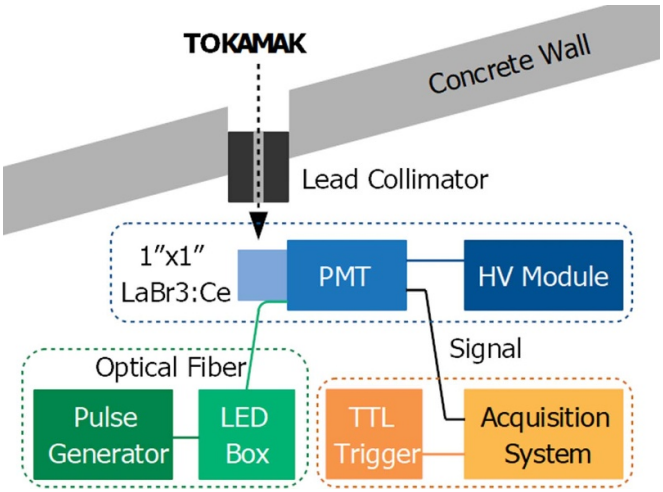

Figure 1. A schematic representation of the REGARDS system. The dotted boxes group the three main components of REGARDS: the HXR detector (in blue), the gain control system (in green) and the acquisition system (in orange).

REGARDS has a dynamic range greater than 20 MeV and an energy resolution of approximately 3% at 661.7 keV. The variation of the system response is limited to a few % for most operational scenarios, see section 3 for details.

This system was initially deployed during the 2019 MST1 runaway electron experimental campaign at the tokamaks AUG and COMPASS and it was successfully employed in the following experimental campaigns. Diagnostic performance and physics results will be discussed in the following sections.

The strict requirements posed by the challenging nature of the runaway electron bremsstrahlung radiation were carefully addressed in the detector design. To facilitate the overview of REGARDS, we can identify three main components of the system: the hard x-ray detector, the gain control system and the acquisition system. Each of them will be discussed in a separate subsection. A schematic representation of the diagnostic can be found in figure 1.

In this picture the dashed arrow represents the collimated line of sight coming from the tokamak to the HXR spectrometer. The blue dotted box encompasses the HXR detector while the green and the orange ones contain the gain control system and the acquisition system, respectively.

2.1. The HXR detector

REGARDS employs a cerium doped lanthanum bromide ($LaBr_3$:Ce) scintillator crystal coupled to a photomultiplier tube (PMT) as HXR detector. Lanthanum bromide was chosen as scintillator material for its fast primary scintillation decay time of approximately 25 ns, mostly based on the experience

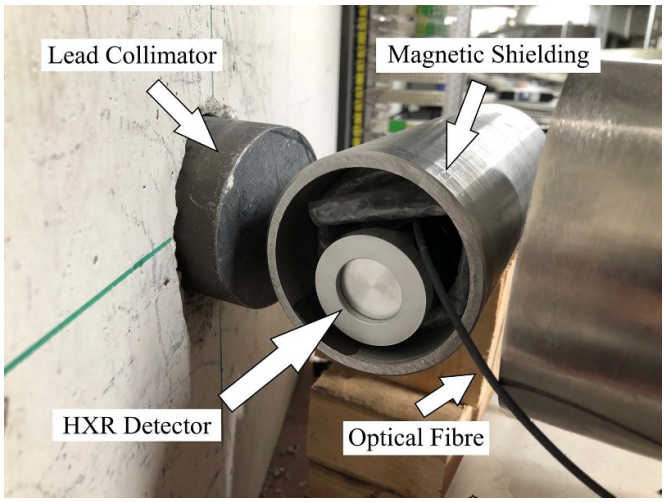

Figure 2. A picture of the HXR detector of REGARDS installed at the ASDEX Upgrade tokamak. The spectrometer is visible in its aluminium casing inside a soft iron cylinder used as magnetic shielding. On the left side of the picture the lead collimator is placed in the line of sight.

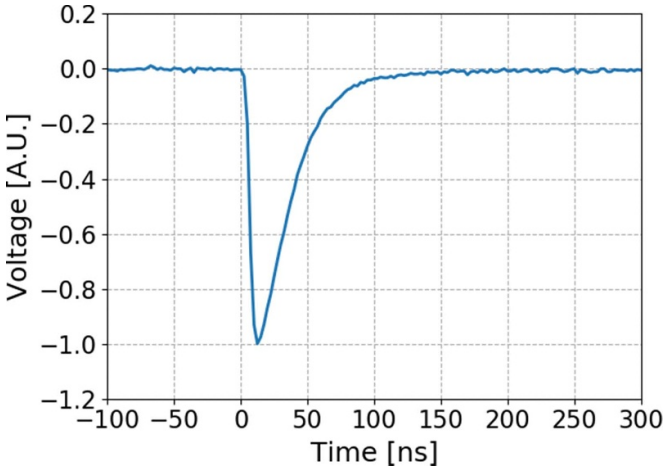

Figure 3. A typical REGARDS HXR signal. The fast pulse shape (FWHM ≈ 30 ns) is essential to reduce events pile-up and to allow operations at MCps counting rates.

with gamma-ray measurements in fast ion experiments at the JET tokamak [17–19]. REGARDS uses a cylindrical crystal of 1 inch in diameter by 1 inch in length manufactured by Saint-Gobain.

At elevated HXR flux levels, two or more HXRs can interact with the scintillation crystal in the same short time interval. Due to the finite scintillation decay time, the resulting signals may accumulate, causing a so-called pile-up event. Although analysis techniques allow to alleviate some of the effects, pile-up generally causes a degradation of the spectrum quality and it is best to be avoided. The fast primary scintillation decay time of $LaBr_3$:Ce ensures a very fast signal necessary to minimize pile-up for the high counting rate operations that it is intended for.

The REGARDS PMT was manufactured by Hamamatsu (model R9420-100-10). It is usually operated at a low bias voltage of approximately −570 V to ensure a broad energy range in excess of 20 MeV and to limit the relative gain shift at high counting rates to less than a few percent.

Tokamaks use intense magnetic fields to confine the plasma. These strong and evolving fields can perturb the behaviour of photomultiplier tubes, which are very sensitive to this kind of disturbance. To mitigate this effect the detector was embedded in two layers of magnetic shielding. The first layer is a μ-metal magnetic shield case produced by Hamamatsu (model E989-03) that completely surrounds the PMT. The second and most external layer consists of a custom-made soft iron cylinder with a thickness of approximately 5 mm that surrounds the entire detector and provides further shielding.

A picture of the HXR detector of REGARDS assembled at the tokamak AUG is shown in figure 2. The tokamak is behind the concrete wall on the left side of the picture. The black cylinder on the left side of the picture is a lead collimator that is often utilized to further diminish the HXR flux, as required in some experimental conditions. A cylindrical aperture through the wall with an outer diameter of 70 mm provides the main collimation element. The detector is visible in the centre of the image in its aluminium casing. The soft iron magnetic shielding cylinder surrounds the detector. Finally, a black optical fibre appears in the lower right part of the picture. This optical fibre is part of the gain control system, discussed in the next subsection.

The detector energy calibration is performed using radioactive gamma-ray sources of known emitted energy. For the calibration of this detector, ^{60}Co and ^{137}Cs were used. The energy resolution of REGARDS HXR detector is approximately 3% at 661.7 keV.

In figure 3(a) typical HXR signal pulse shape measured by REGARDS is presented. The use of a fast inorganic scintillator in conjunction with a PMT allows for a very fast signal of approximately 100 ns. The full width at half-maximum of the signal is approximately 30 ns. This fast detector reduces the effects of pile-up and allows for HXR spectroscopy even at the high counting rates (up to a few MCps) in runaway electron discharges.

Figure 4 shows a signal time trace recorded during a plasma discharge with counting rates greater than 1 MCps. As visible from the picture, due to the fast pulse shape only a few pulses suffer from pile-up as a consequence of the high HXR counting rate. Moreover, even when affected by pile-up, most of the individual pulses are still easily recognizable and their amplitude can be restored using dedicated pile-up recovery algorithms.

2.2. The gain control system

There are two main effects that can modify the detector gain during runaway electron bremsstrahlung measurements. The first one is caused by the residual unshielded tokamak magnetic field interacting with the PMT and interfering with its multiplication stage. The second effect is caused by the PMT non-linear response as the current from the signal approaches the bias current. This last effect can become non negligible for runaway electron scenarios with MCps counting rates.

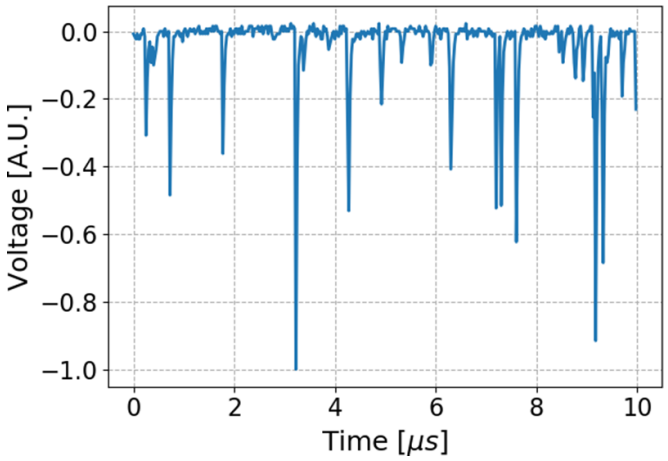

Figure 4. A typical signal time trace recorded during a high counting rate (>1 MCps) phase of a plasma discharge. A limited number of pile-up events are visible and all signals are still recoverable using pile-up recovery algorithms.

An external control system was developed to monitor the detector gain during the plasma discharge. This system is made of a blue light-emitting diode (model NSPB500AS by Nichia) mounted in a light-tight box, an electrical pulse generator (model 577 by Berkeley Nucleonics) and an optical fibre. The pulse generator is used to pilot the LED which is periodically fired at constant bias voltage. The light emitted by the LED is then transported to the PMT photocathode by the optical fibre. The parameters of the electrical pulse generator are adjusted such that the light emitted by the LED mocks the scintillation of a high energy photon interacting with the $LaBr_3$:Ce crystal. For these experiments, we chose to fire the LED at a constant rate of 10 kHz with an equivalent HXR energy of approximately 12.5 MeV.

These LED pulses are acquired at the same time of the plasma discharge and then separated from the HXR signals using pulse shape discrimination techniques during off-line analysis. By comparing the amplitude of the LED pulses during the time of the discharge it is possible to quantify the gain shift of the diagnostic. If needed, this information can be used to perform offline corrections for small gain shifts below 10%.

2.3. The acquisition system

A crucial role in REGARDS performance is played by the acquisition system. Due to the very high rate of the HXR events associated with runaway electron bremsstrahlung, it is preferable to acquire data in a continuous acquisition stream instead of operating with a triggered mode. This technique prevents loss of data due to the acquisition dead time and facilitates pile-up detection and recovery.

The acquisition system used for REGARDS is an ADC model NI5772 with PXIe-7976 FlexRIO module by National Instruments. This system allows for continuous data collection at a 400 MHz sampling rate for more than 10 s, which exceeds the duration of the heating phase for most tokamaks without superconducting magnets, such as ASDEX Upgrade or COMPASS.

The data acquisition is started with an external transistor–transistor logic trigger to ensure synchronisation with the plasma discharge and other diagnostics. Data is stored in non-volatile memory in the time between two plasma discharges, that are usually tens of minutes apart.

3. Diagnostic performance

REGARDS was first employed during the 2019 MST1 AUG runaway electron experimental campaign. The detector was installed along a radial line of sight of the tokamak, outside the torus hall, as shown in figures 1 and 2. The AUG torus hall wall is made of concrete and is 2 meters thick, providing good shielding from background radiation. The distance between the detector and the magnetic axis of the machine is approximately 11 meters. The line of sight is defined by a lead collimator inside the torus hall. To further limit the HXR flux on the detector an additional lead collimator with a cylindrical aperture of 10 mm in diameter and 100 mm thick was placed in front of the detector as shown in figure 2.

3.1. Runaway electron bremsstrahlung radiation

During a typical AUG runaway electron discharge the REGARDS acquisition time is set to 10 s, starting at the very beginning of the plasma discharge ($t = 0$ s). The runaway electron event is usually triggered approximately at $t = 1$ s through a massive gas injection [10]. The generated runaway beam typically lasts for a few hundreds of milliseconds before confinement is lost or the beam is terminated. Figure 5 shows the plasma current measured during one of these experiments, AUG shot #35 887. In the first part of the discharge the plasma current steadily increases up to a desired value of 760 kA. At $t = 1$ s a plasma disruption is triggered using a massive gas injection of argon and a runaway electron beam is formed. In figure 5 the current measured after the plasma disruption ($t >$ 1.01 s) represents the runaway electron beam current.

After the massive gas injection, the newly formed runaway electron beam interacts with the post disruption plasma and emits radiation. The HXR spectrum of the runaway electron bremsstrahlung radiation collected by REGARDS during the entire time of the discharge is shown in figure 6 (in blue). The bin energy step is 100 keV. The bremsstrahlung spectrum is continuous, with a shape that is mostly exponential and reaches energies up to 10 MeV. Due to the nature of bremsstrahlung emission, this suggests that a fraction of the runaway electrons in the beam in shot #35 887 reached energies greater than 10 MeV.

A more detailed analysis of this HXR spectrum is presented in section 4.

3.2. Detector stability

During off-line analysis, the HXR events can be separated from the LED pulses of the control monitor system using pulse shape discrimination algorithms. By isolating the LED pulses and studying their behaviour during the discharge, we can infer the detector gain stability. The typical duration of a runaway

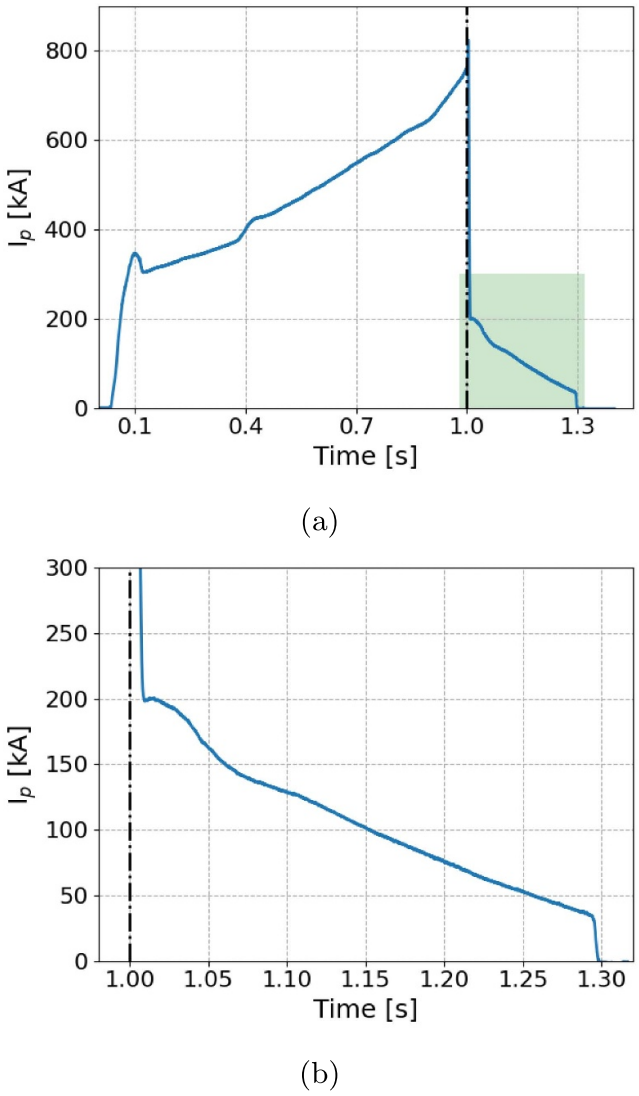

Figure 5. (a) AUG plasma current during a runaway experiment (discharge #35 887). After the disruption triggered by a massive Ar gas injection at $t = 1$ s a 200 kA runaway beam is formed. The duration of the runaway electron beam is about 300 ms.
(b) Enlargement of the plasma current in the light green area of (a), corresponding to the RE phase of the discharge.

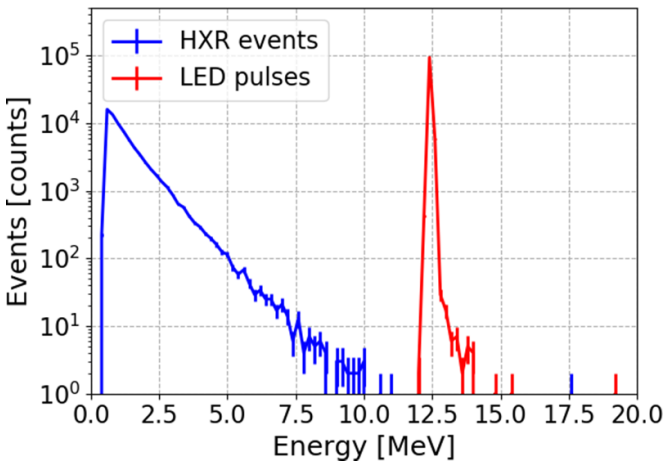

Figure 6. A RE bremsstrahlung spectrum measured at AUG using REGARDS (blue) in discharge #35 887. Data are inegrated over the whole discharge. The exponential spectrum reaches energies up to 10 MeV. The gain control system LED pulses collected during the discharge form the red peak at 12.5 MeV.

experiment discharge at AUG is under 2 s. After $t = 5$ s we assume the PMT gain to be stable, since by that time no residual magnetic field or HXR radiation are present. We compute the mean LED energy by averaging LED events over this time window ($5\,\text{s} \leqslant t \leqslant 10\,\text{s}$) and we use this value as a reference for the unbiased gain. When unperturbed, the coefficient of variation of the LED events is $\sigma/\mu = 0.34\%$ which corresponds to a LED energy resolution of approximately 0.8% at 12.5 MeV. Here μ is the average LED energy ($\mu = 12.5$ MeV) and σ is the standard deviation of the measured LED energies ($\sigma = 0.042$ MeV). We can estimate the detector gain shift by looking at the relative deviation of LED events from the reference value during the plasma discharge.

In figure 7(a) the LED events during the plasma discharge are shown as the relative deviation from this computed mean for AUG discharges #35 887 and #35 891. Both are MGI discharges but with different RE current resulting in different counting rates of the HXR radiation measured by REGARDS. In figure 7(b) a Savitzky–Golay filter is applied to the data to highlight the behaviour of the detector gain (solid line). At the beginning of the discharges, from$t=$ 0 s up to$t\approx$ 1 s, we can see a linear increase in the gain shift, up to 0.8% for discharge #35 887 and up to 1.0% for discharge #35 891. This effect is caused by the steady build-up of the plasma current and thus of the tokamak magnetic field in the initial phase of the discharge. After this initial phase, a sudden increase in the gain shift is clearly visible corresponding to the runaway electron generation triggered by the massive gas injection, at $t =$ 1.008 s for discharge #35 887 and at $t = 1.186$ s for discharge #35 891 respectively. This shift is caused by the PMT nonlinearity at high currents caused by the high HXR flux on the detector and stays below 3% for most time points. The maximum HXR counting rates measured were 0.48 MCps for discharge #35 887 and 1.23 MCps for discharge #35 891. Finally, after the short runaway electron phase, the system gain returns to the original unperturbed value in a few seconds.

Figure 8 shows the HXR events counting rate for discharge #35 887 as a function of time. Each bin of the counting rate time trace contains 3000 HXR events. At $t=$ 1.008 s the runaway event is triggered by the massive gas injection. Figure 9 shows a comparison between the HXR counting rate (in blue) and the relative detector gain shift (in red) during the time of the runaway electron event for discharge #35 887. A clear correlation between the two curves is visible. The temporal delay in the relative gain shift of approximately 13 ms is due to the finite response time of the detector to the current changes. This plot exemplifies the effect that high counting rates can have on the data quality and highlights the importance of monitoring the detector gain using the gain control system. A more complete discussion on the high rate limitations of the REGARDs system is presented in section 5.

The data collected during the runaway electron campaigns at AUG demonstrated the stability of REGARDS under severe

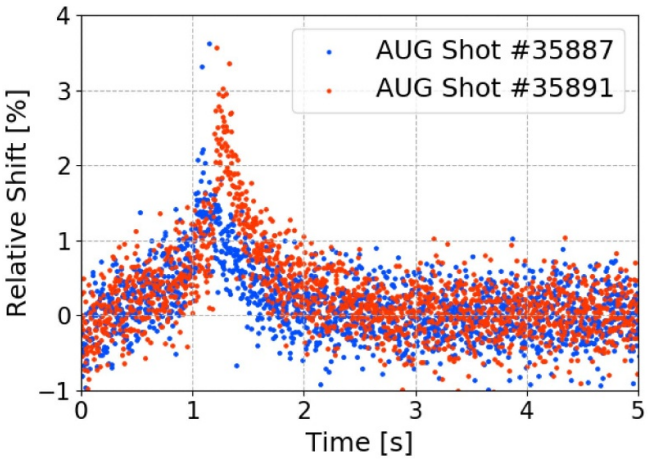

(a)

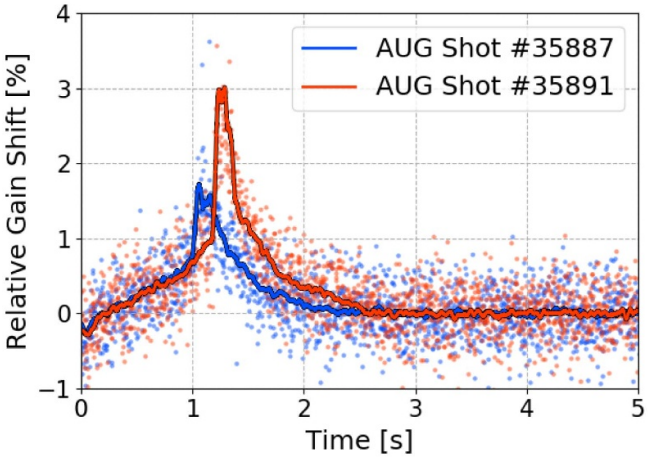

(b)

Figure 7. (a) The LED pulses collected during the plasma discharge presented as the relative shift from the unperturbed reference value for two different AUG discharges. (b) A Savitzky–Golay filter is applied to the same datasets to highlight the detector gain shift. Before the massive gas injection (at $t = 1.008$ s and at $t = 1.186$ s for discharges #35 887 and #35 891 respectively) a linear increase in the detector gain is caused by the increasing tokamak magnetic field. The sharp spike of the detector gain shift after the MGI is caused by the PMT non-linearity at high HXR counting rate. A slow recovery of the gain can be appreciated after the RE phase. The gain shift is $<3\%$ at counting rates in excess of 1 MCps.

HXR fluxes associated with runaway electron emission, as its gain shift was lower than 3% at high counting rates exceeding 1 MCps.

4. HXR spectra analysis

REGARDS high performance allows characterizing the runaway electron beam evolution extracting information from the high energy component of the emitted bremsstrahlung radiation. In this section, we present the analysis of AUG shot #35 887 to exemplify the technique.

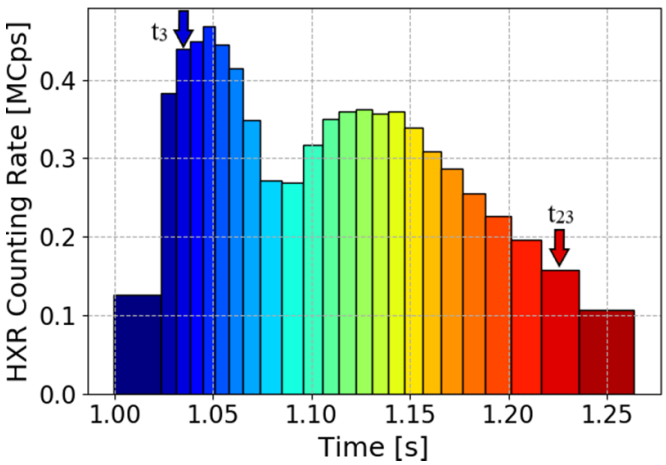

Figure 8. The HXR counting rate during discharge #35 887 at AUG. Each bin contains 3000 events. The arrows indicate the two time windows selected to showcase a typical analysis of the shot in section 5.

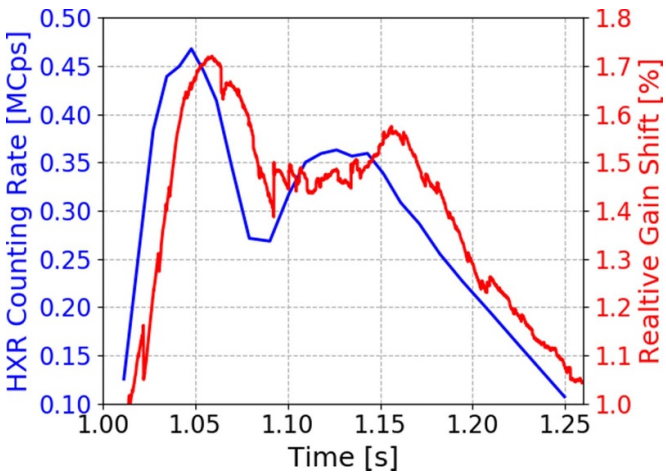

Figure 9. A comparison between the HXR counting rate (in blue) and the detector relative gain shift (in red) after the massive gas injection in shot #35 887. A clear correlation between the two curves is visible, highlighting the effect of high counting rates on the detector stability and the importance of REGARDS gain control system for these high counting rate measurements.

To characterize the evolution of the runaway electron beam, the measured HXR events are split in different time segments. For each time segment an energy spectrum of the runaway electron bremsstrahlung radiation is produced integrating the HXR events measured in that temporal region. Finally, each spectrum is analyzed to extract information on the runaway electron evolution during the discharge. For the analysis of AUG shot #35 887, the HXR events collected during the runaway electron phase of discharge were split into 24 time windows, each one containing 3000 events, as shown in figure 8. The time windows were adjusted to obtain a constant event population inside each bin. The bin population was chosen to ensure good HXR spectrum statistics without compromising the time resolution. To facilitate discussion, data belonging to each time window will be presented with the same colour coding used in figure 8.

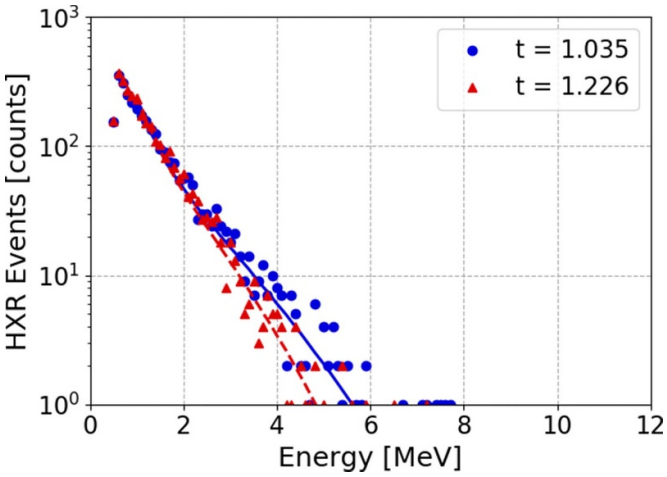

Figure 10. HXR spectra at two different stages of the RE beam evolution. The bin energy step is 100 keV. Each spectrum contains 3000 HXR counts. At the beginning of the RE phase the bremsstrahlung spectrum (blue dots) is more energetic than the one at the end of the discharge (red triangles), suggesting a similar evolution of RE beam maximum energy.

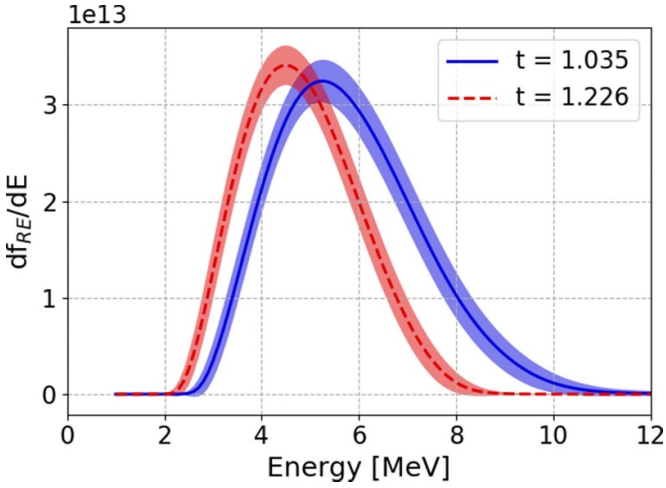

Figure 11. Reconstructed RE energy distribution functions for two different stages of the RE phase in discharge #35 887. First-order Tikhonov regularization algorithm was used to recover this information from the two measured HXR spectra in figure 10. The algorithm ensures smooth non-negative solutions.

The HXR spectra for time windows $t_3 = 1.035$ s and $t_{23} = 1.226$ s are shown in figure 10 (blue dots and red triangles, respectively). These two spectra refer to different moments of the runaway electron beam evolution. The first one, t_3, is collected during the runaway electron beam formation while the second one, t_{23}, is closer to the end of the beam duration. Information on the runaway electron beam can be already inferred by noticing that the t_3 spectrum has a significantly larger number of events at higher energies than t_{23}. This suggests a more energetic beam at $t = t_3$ and a less energetic beam at $t = t_{23}$.

More detailed information can be obtained by modelling the detector response and the RE bremsstrahlung emission and using deconvolution techniques to infer the underlying runaway electron energy distribution function from the measured HXR spectrum. The Monte Carlo code MCNP [20] was used to model the detector response function for various monoenergetic HXR energies, while the code GENESIS [21, 22] was utilized to model the runaway bremsstrahlung emission in the HXR energy range.

This deconvolution process is in practice an ill-posed problem, i.e. several different runaway energy distribution functions could explain the same measured HXR spectrum within the bounds of the experimental error. A common technique to address this problem is to use deconvolution algorithms such as Tikhonov regularization, single value decomposition or Richardson–Lucy deconvolution to guide the selection of the solution with some prior knowledge of its features, such as smoothness or non-negativity. For a detailed analysis of the performance of these algorithms on this specific problem see [9].

For our analysis we use the non-negative first-order Tikhonov reconstruction, which was applied to the data of each of the 24 time windows. For this type of unfolding, opting for a first-order deconvolution leads to a solution that is smoother and physically plausible. Figure 11 shows the calculated runaway electron energy distribution functions for $t = t_3$ and $t = t_{23}$. The shaded area represents a 1–σ confidence interval in the reconstruction. We can notice that the runaway energy distribution at $t = t_3$ has higher average energy than the distribution at $t = t_{23}$. Moreover, the high energy tail of the $t = t_3$ distribution is significantly more populated than the $t = t_{23}$ one. This confirms in a more quantitative way the previous observation on the runaway electron energy evolution we made by inspection of the HXR spectra.

Another parameter that can be extracted from these reconstructed RE energy distributions, and that is of great interest to describe the runaway electron evolution, is represented by the maximum energy of the beam. This parameter, referred here as E^*_{RE}, is the energy value at which the cumulative runaway electron energy distribution is equal to 90%, namely:

$$F_{\mathrm{RE}}(E^*_{\mathrm{RE}}) = \int_0^{E^*_{\mathrm{RE}}} f_{\mathrm{RE}}(E)\, dE = 0.9$$

where f_{RE} is the normalised runaway electron energy distribution.

Figure 12 shows the time evolution of E^*_{RE} during the AUG plasma discharge #35 887. A clear evolution of the runaway electron beam maximum energy is visible, with an initial increase of the beam maximum energy at the early stages of the beam formation and a subsequent and almost linear fall in the second half of the beam duration.

Information like the one presented in figure 12 is the only way, besides synchrotron radiation measurements in some cases [23], to of the RE energies and

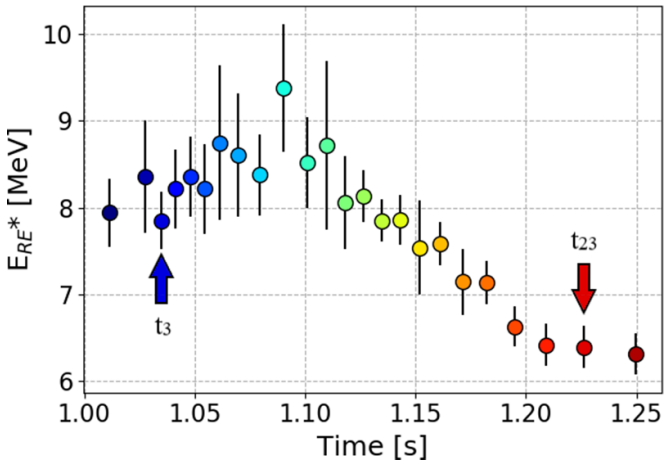

Figure 12. Maximum energy of the runaway electron beam during AUG discharge #35 887. A clear evolution of this parameter is visible. A small increase at the beginning of the RE phase is followed by an almost linear decrease in the maximum energy.

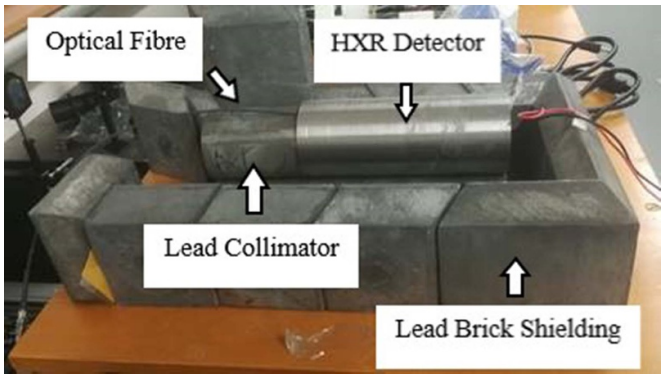

Figure 13. REGARDS detector setup at COMPASS. At the centre of the picture the soft iron cylinder used for magnetic shielding is visible. At its left, the cylindrical lead collimator and the black optical fibre are visible. Lead bricks were used to shield the detector from the background radiation.

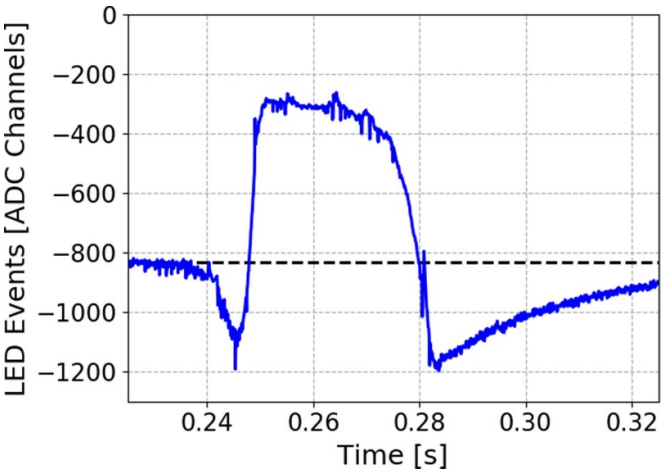

Figure 14. Time trace of the digitized LED pulses in the discharge #19 979 at COMPASS. Only the maximum amplitude of each individual LED pulse is shown as a blue point on the graph. The average value of the unperturbed digitized LED events is shown in by the black dashed line. A clear deviation from the unperturbed value is visible during the runaway electron phase of the discharge.

the impact that alternative mitigation techniques have on them. For a more detailed analysis of the AUG discharges see [24].

5. REGARDS performance at extremely high HXR fluxes

One of the main characteristics of REGARDS is portability. The entire system was designed to be compact and easily transferable to be installed and used at different tokamak facilities. In January 2020 REGARDS was installed at the medium-size tokamak COMPASS to collect preliminary data and test the detector performance at extremely high HXR fluxes. Extremely high fluxes were expected at COMPASS due to the proximity of the detector to the machine and the lack of an already existing collimated line of sight. The detector was shielded on site against background radiation using multiple lead blocks as shown in figure 13.

The tests performed at COMPASS were particularly useful to test the robustness of the gain control system of REGARDS, under extremely high rates of several MCps. A good example to highlight the behaviour of REGARDS under these challenging conditions is discharge #19 979. During this shot REGARDS measured high HXR fluxes, with counting rates exceeding 10 MCps. Figure 14 shows the time trace of the digitized LED pulses during the discharge. To enhance readability, only the maximum amplitude of each individual LED pulse is shown. If no gain shift occurs, we expect the LED pulse amplitude to be constant in time within the statistical deviation presented in paragraph 3.2. The average value of the unperturbed digitized LED events corresponds to approximately −830 ADC channels and it is shown in figure 14 by the black dashed line. A clear deviation of the LED pulse amplitude from the unperturbed value is visible during the discharge. Figure 15 shows the computed relative gain shift from the unperturbed value for the same discharge. In the first phase of discharge #19 979, the detector gain increases under the influence of the magnetic field and the HXR high rate. In this initial phase a very high shift in excess of +40% was reached caused by an extreme HXR counting rate of 5 MCps at t= 0.245 s. After this point the HXR flux increased even more resulting in a sharp gain drop. During this second phase, the gain shift dropped below a value of −60% under an estimated HXR rate in excess of 10 MCps. The progressive detector gain recovery is visible only after the termination of the runaway electron phase ($t = 0.283$ s).

By inspecting figure 15, we find that a gain shift of +10% is reached when the counting rate is approximately 3 MCps (at $t = 0.242$ s). Considering that event amplitude correction

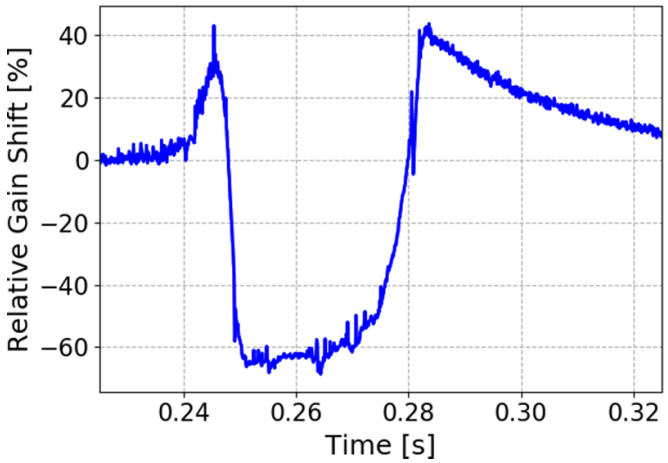

Figure 15. Detector relative gain for discharge #19 979 at COMPASS. In the first phase of discharge the detector gain increases under the influence of the magnetic field and the HXR high flux up to $+40\%$ at $t = 0.245$ s. Later the detector gain sharply dropped below a value of -60% under an estimated HXR rate in excess of 10 MCps. Detector gain recovery is visible after the termination of the runaway electron phase at $t = 0.283$ s.

may be more difficult when the gain shift exceeds 10%, we take 3 MCps as the upper limit for robust measurements of the RE energies with REGARDS.

6. Discussion

An important aspect of a diagnostic system aimed at characterizing the time evolution of the runaway electron energy distribution is time resolution. REGARDS time resolution is limited by the HXR event statistics. If too few HXR events are detected during the discharge the integration time window must be increased to allow a significant number of counts in the HXR spectrum. This effect, limited to very low energy or extremely short beams, reduces the capability of capturing the fast components in the evolution of the runaway electron distribution function. A careful balance in the design of the detector position and collimation is therefore of extreme importance to allow for a desirable operation range with counting rates from 0.1 MCps to 3 MCps at most. This careful evaluation was performed for the AUG line of sight with the help of a MCNP Monte Carlo model, which allow for simulation of the HXR transport and attenuation. The design of the lead collimator shown in figures 1 and 2 was based on these calculations. The management of the incident HXR flux at AUG allowed for time resolutions of approximately 10 ms, that we deem sufficient for studying the evolution of the RE energy distribution function.

The tests performed at COMPASS showcase the complexity of RE bremsstrahlung measurements and the importance of the REGARDS gain control system. Severe HXR flux can drastically change the detector gain and behaviour. Without the external LED reference signal it would have been extremely difficult to ascertain if the variations in the measured HXR spectrum during the discharge were caused by a detector gain shift or by a real change in the underlying runaway electron distribution function. Moreover, the gain control system gives an immediate and quantitative indication of the detector stability during the discharge and thus of the data quality. Finally, this example highlights the importance of collimation to reduce the severe runaway electron HXR fluxes and to ensure that the detector runs within the boundaries of its operational domain.

7. Conclusion

A new fast HXR detector optimized for runaway electron bremsstrahlung measurements was developed: the REGARDS. REGARDS was firstly deployed during the 2019 AUG MST1 runaway electron campaign and worked as designed. The system proved to be fast (enabling measurements of the RE energies with <10 ms temporal resolution) and stable (relative gain shift relative shift below 3% with HXR counting rates in excess of 1 MCps). The system energy range is from a few hundreds keV to more than 20 MeV with an energy resolution of 3% at 661.7 keV. REGARDS is a portable device and it was also tested at COMPASS during the 2019 MST1 runaway electron campaign to ascertain the system limitations under extreme HXR fluxes. These tests proved the importance and the robustness of the REGARDS gain control system, and the need to monitor this parameter for reliable measurements of the RE energy.

REGARDS allowed reconstruction of the runaway electron distribution function in the AUG MST1 runaway electron campaign with time resolutions of approximately 10 ms. Important quantities, such as the average and maximum energy of the RE beam, can be extracted and evaluated at different times of the discharge. This information is a crucial contribution to first-principle model validation and quantitative assessment of RE mitigation techniques.

REGARDS has now become an established diagnostic for mid-sized tokamaks of the EUROfusion program, such as AUG, where it contributes to studies of the runaway electron distribution function in mitigation experiments.

Data availability statement

The data cannot be made publicly available upon publication because they are not available in a format that is sufficiently accessible or reusable by other researchers. The data that support the findings of this study are available upon reasonable request from the authors.

Acknowledgments

This work has been carried out within the framework of the EUROfusion Consortium and has received funding from the Euratom research and training programme 2014–2018

under Grant Agreement No. 633053. The views and opinions expressed herein do not necessarily reflect those of the European Commission.

ORCID iDs

A Dal Molin https://orcid.org/0000-0003-0471-1718
M Nocente https://orcid.org/0000-0003-0170-5275
D Rigamonti https://orcid.org/0000-0003-0183-0965
M Tardocchi https://orcid.org/0000-0001-7771-9521
A Shevelev https://orcid.org/0000-0001-7227-8448
E Khilkevitch https://orcid.org/0000-0001-7995-3645
M Iliasova https://orcid.org/0000-0003-3170-1507
L Giacomelli https://orcid.org/0000-0002-3230-969X
G Gorini https://orcid.org/0000-0002-4673-0901
E Perelli Cippo https://orcid.org/0000-0002-8151-3427
F D'Isa https://orcid.org/0000-0002-2486-5602
G Papp https://orcid.org/0000-0003-0694-5446
E Macusova https://orcid.org/0000-0002-0381-9244
J Cerovsky https://orcid.org/0000-0001-6051-4001
O Ficker https://orcid.org/0000-0001-6418-9517
M Salewski https://orcid.org/0000-0002-3699-679X
V Kiptily https://orcid.org/0000-0002-6191-7280

References

[1] Boozer A H 2015 Theory of runaway electrons in ITER: equations, important parameters and implications for mitigation *Phys. Plasmas* **22** 032504
[2] Boozer A H 2017 Runaway electrons and ITER *Nucl. Fusion* **57** 056018
[3] Sweeney R *et al* 2020 MHD stability and disruptions in the SPARC tokamak *J. Plasma Phys.* **86** 865860507
[4] Hender T C *et al* 2007 Chapter 3: MHD stability, operational limits and disruptions *Nucl. Fusion* **47** S128–202
[5] Reux C *et al* 2022 Physics of runaway electrons with shattered pellet injection at JET *Plasma Phys. Control. Fusion* **64** 034002
[6] Pautasso G *et al* 2020 Generation and dissipation of runaway electrons in ASDEX upgrade experiments *Nucl. Fusion* **60** 086011
[7] Ficker O *et al* 2019 Runaway electron beam stability and decay in COMPASS *Nucl. Fusion* **59** 096036
[8] Mlynar J *et al* 2018 Runaway electron experiments at COMPASS in support of the EUROfusion ITER physics research *Plasma Phys. Control. Fusion* **61** 014010
[9] Panontin E *et al* 2021 Comparison of unfolding methods for the inference of runaway electron energy distribution from γ-ray spectroscopic measurements *J. Instrum.* **16** C12005
[10] Pautasso G *et al* 2016 Disruption mitigation by injection of small quantities of noble gas in ASDEX upgrade *Plasma Phys. Control. Fusion* **59** 014046
[11] Gobbin M *et al* 2017 Runaway electron mitigation by 3D fields in the ASDEX-upgrade experiment *Plasma Phys. Control. Fusion* **60** 014036
[12] Gobbin M, Valisa M, White R, Cester D, Marrelli L, Nocente M, Piovesan P, Stevanato L, Puiatti M and Zuin M 2016 Runaway electron mitigation by applied magnetic perturbations in RFX-mod tokamak plasmas *Nucl. Fusion* **57** 016014
[13] Lvovskiy A, Paz-Soldan C, Eidietis N, Molin A D, Nocente M, Cooper C, Rigamonti D, Tardocchi M and Taussig D 2022 Upgrades to the gamma ray imager on DIII-d enabling access to high flux hard x-ray measurements during the runaway electron plateau phase *Rev. Sci. Instrum.* **93** 113524
[14] Dal Molin A *et al* 2021 Novel compact hard x-ray spectrometer with MCps counting rate capabilities for runaway electron measurements on DIII-d *Rev. Sci. Instrum.* **92** 043517
[15] Dal Molin A, Martinelli L, Nocente M, Rigamonti D, Abba A, Giacomelli L, Gorini G, Lvovskiy A, Muraro A and Tardocchi M (JET Contributors) 2018 Development of a new compact gamma-ray spectrometer optimised for runaway electron measurements *Rev. Sci. Instrum.* **89** 10I134
[16] Nocente M *et al* 2018 High resolution gamma-ray spectrometer with MHz capabilities for runaway electron studies at ASDEX upgrade *Rev. Sci. Instrum.* **89** 10I124
[17] Nocente M *et al* 2019 MeV range particle physics studies in tokamak plasmas using gamma-ray spectroscopy *Plasma Phys. Control. Fusion* **62** 014015
[18] Eriksson J *et al* 2015 Dual sightline measurements of MeV range deuterons with neutron and gamma-ray spectroscopy at JET *Nucl. Fusion* **55** 123026
[19] Nocente M *et al* 2013 High resolution gamma ray spectroscopy at MHz counting rates with $LaBr_3$ scintillators for fusion plasma applications *IEEE Trans. Nucl. Sci.* **60** 1408–15
[20] Werner C J *et al* 2018 Mcnp6.2 release notes, report la-ur-18-20808 Los Alamos National Laboratory
[21] Nocente M 2012 Neutron and gamma-ray emission spectroscopy as fast ion diagnostics in fusion plasmas *PhD Thesis* Università degli Studi di Milano-Bicocca
[22] Nocente M *et al* 2017 Conceptual design of the radial gamma ray spectrometers system for α particle and runaway electron measurements at iter *Nucl. Fusion* **57** 076016
[23] Hoppe M, Embréus O, Tinguely R, Granetz R, Stahl A and Fülöp T 2018 SOFT: a synthetic synchrotron diagnostic for runaway electrons *Nucl. Fusion* **58** 026032
[24] Shevelev A *et al* 2021 Study of runaway electron dynamics at the ASDEX upgrade tokamak during impurity injection using fast hard x-ray spectrometry *Nucl. Fusion* **61** 116024